



FULL PAPER

Synthesis, biological evaluation, and in silico study of pyrazoline-conjugated 2,4-dimethyl-1H-pyrrole-3-carboxylic acid derivatives

Nishant K. Rasal | Rahul B. Sonawane | Sangeeta V. Jagtap

Department of Chemistry, Baburaoji Gholap College, Affiliated to Savitribai Phule Pune University, Pune, India

Correspondence

Sangeeta V. Jagtap, Department of Chemistry, Baburaoji Gholap College, Affiliated to Savitribai Phule Pune University, Pune 411017, India.
Email: sangeetajagtap@rediffmail.com

Abstract

A potential molecular hybridization strategy was used to develop 24 novel pyrazoline-conjugated 2,4-dimethyl-1H-pyrrole-3-carboxylic acid and amide derivatives. The preliminary in vitro antimicrobial assay delivered four potential derivatives with growth inhibition in the range of 50.87–56.60% at the concentration of 32 µg/ml. In the search of an anticancer candidate, all derivatives were screened by NCI-60 at 10 µM concentration, revealing that 12 derivatives were potential agents against the various types of cancer cell lines, with growth inhibition in the range of 50.21–108.37%. The in vitro cytotoxicity assay against the cell line HEK293 (human embryonic kidney cells) and the hemolysis assay of the representative potent compounds propose their potential for a good therapeutic index. In silico studies of the most potent derivatives qualified their significant pharmacokinetic properties with good predicted oral bioavailability and their adherence to Lipinski's rule of five for druglikeness. A molecular docking study against VEGFR-2 with the best-scored conformations reinforced their anticancer potency. The docking study of the most potent compound against VEGFR-2 with the best-scored conformations displayed a binding affinity (–9.5 kcal/mol) comparable with the drug sunitinib (–9.9 kcal/mol) and exhibited that tighter interactions at the active adenosine triphosphate site might be responsible for anticancer potency.

KEYWORDS

2,4-dimethyl-1H-pyrrole, antimicrobial, antiproliferation, drug discovery, molecular docking

1 | INTRODUCTION

Under the healthy condition of the body, the number and growth of each type of cell follow a highly controlled mechanism. However, any wrong signal through the alteration of genes directly affects the cell life cycle and it leads to continuous uncontrolled multiplication, which results in the accumulation of abnormal cells in the form of a mass of malignant cells called "cancer."^[1] Worldwide, at present, cancer ranks first for the mortality and morbidity, and it is estimated that almost 22 million people may be affected from it by 2030.^[2] According to the World Health Organization (WHO), in the year

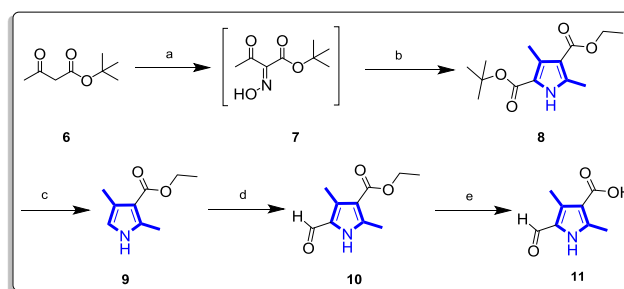
2018, 18.1 million cancer patients were found as new cases and almost 9.6 million died from the disease. By 2040, the figure for new cancer patients will rise to 29.4 million.^[3] To get relief from cancer at an early stage, the application of chemotherapy is the most popular approach, but it has several unbearable side effects on bone marrow, the gastrointestinal tract, hair, and so forth, and it directly affects an individual's physical health and quality of life.^[4] Hence, myriad efforts have been made by researchers to develop a new anticancer agent with minimum side effects.

The topmost potential anticancer molecules semaxanib, obatoclox, sunitinib, toceranib, and so on, exhibited 2,4-dimethyl-1H-pyrrole

moiety as a key building block along with the 2-indoline ring. Further exploration of this skeleton delivered various significant derivatives, **1**,^[5] **2**,^[6] **3**,^[7] and so on, which exhibited the antiproliferative activity comparable with sunitinib against various cancer cell lines. Many researchers have endeavored to find various amide functionalities at the 3-position of pyrrole along with structural modification on the 2-indoline ring (Figure 1).

In medicinal chemistry, 2-pyrazoline acts as a privileged scaffold due to its presence in numerous important medical and biochemical agents that have been effectively utilized as antibacterial, antifungal, anti-inflammatory, analgesic, antiparasitic, antiviral, antitubercular, anticancer, anesthetic, and insecticidal agents.^[8–22] Recently, a 4,5-unsaturated pyrazoline ring called pyrazole has marked its versatile use in the drug design, and it has been found to have a remarkable presence in various potential anticancer molecules such as celecoxib, SC5584. Liu et al.^[23] have confirmed that celecoxib induces apoptosis in the human osteosarcoma cell line and enhances the cytotoxic effect of cisplatin.^[23] Celecoxib reduces the risk of manifestation and growth of the various types of cancers, especially breast cancer.^[24] Besides, pyrazoline motifs were reported as potent EGFR inhibitors **4** and **5**,^[25,26] aurora kinase inhibitors,^[27] telomerase inhibitors,^[28] tubulin assembly inhibitors,^[29] and so forth (Figure 1).

In our earlier work, 2,4-dimethylpyrrole-conjugated chalcone derivatives were delivered as the potential scaffold for further development.^[30] Hence, as an extension of the previous work and in the continuous search of novel antimicrobial and anticancer templates,^[31] this study presents the new hybrid skeleton consisting of 2,4-dimethylpyrrole moiety clubbed with the 2-pyrazoline ring. The hybrid skeleton was further explored by the screening of a series of derivatives for in vitro antimicrobial and anticancer activity.



SCHEME 1 The synthesis of scaffold **11**. Reagents and conditions: (a) NaNO_2 , AcOH , RT, 3 hr; (b) ethyl acetoacetate, Zn powder, AcOH , 65°C , 3 hr; (c) HCl , EtOH , 70°C , 3 hr; (d) dimethylformamide, POCl_3 , dichloromethane, reflux, 2 hr; (e) KOH , H_2O , MeOH , reflux, 5 hr

2 | RESULTS AND DISCUSSION

2.1 | Chemistry

The scaffold 5-formyl-2,4-dimethyl-1*H*-pyrrole-3-carboxylic acid (**11**) was synthesized according to Scheme 1 adopted from the literature.^[32] The chalcone derivatives **12a–c** were prepared by the Knoevenagel condensation and subjected to acid–amine coupling using TBTU as a coupling reagent to get the desired derivatives **13a–c** as per the previously reported synthetic procedure.^[30] The targeted alkyl- or aryl-substituted pyrazoline–pyrrole derivatives **14a–i**, **15a–c**, **15f–h**, and **15k–m** were prepared by treatment of respective chalcones with hydrazine HCl derivatives in the presence of NaOH and ethanol under reflux conditions (Scheme 2). For the remaining acyl-substituted pyrazoline–pyrrole derivatives (compounds **15d**, **15e**, **15i**, **15j**, **15n**, and **15o**), chalcone was interacted with the hydrazine hydrate to get a basic pyrazoline compound, which was further acylated using the respective acyl chloride.

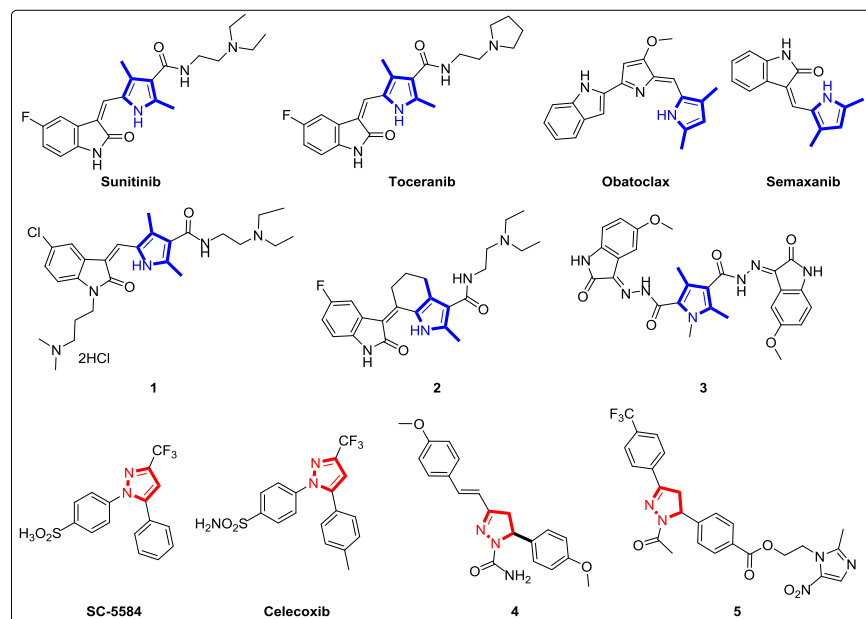
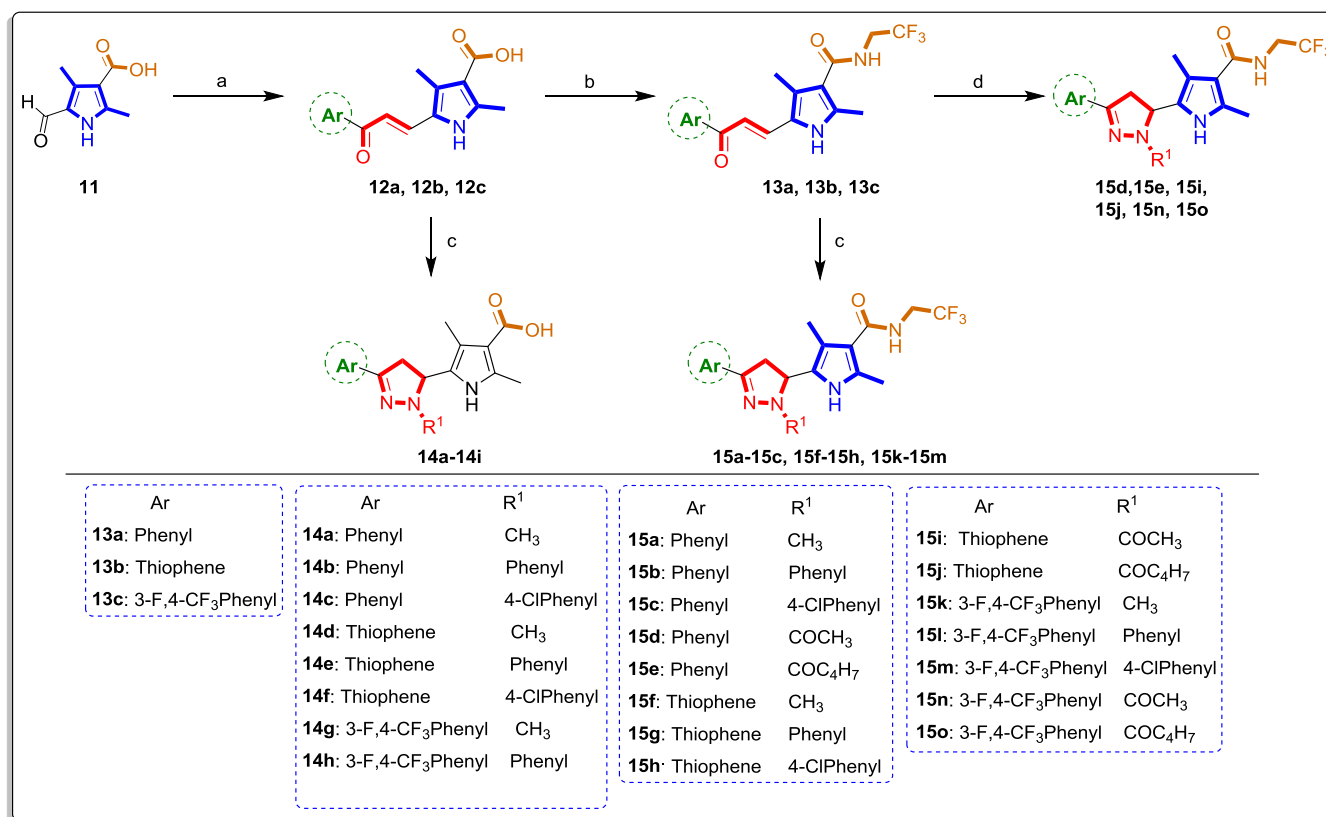


FIGURE 1 Reported 2,4-dimethyl-1*H*-pyrrole and pyrazoline-containing anticancer compounds



SCHEME 2 The synthesis of target compounds **13a–c**, **14a–i**, and **15a–o**. Reagents and conditions: (a) ArCOCH₃, KOH, MeOH, RT, 48 hr; (b) CF₃CH₂NH₂ HCl, DIPEA, TBTU, DMF, RT, 24 hr; (c) R¹NHNH₂ HCl, NaOH, EtOH, reflux, 2 hr; (d) (i) N₂H₄, EtOH, H₂O, reflux, 2 hr, (ii) R¹COCl, TEA, CHCl₃, RT, 2 hr. DIPEA, *N,N*-diisopropylethylamine; DMF, dimethylformamide; TEA, triethylamine

The formation of the pyrazoline ring was confirmed by ¹H nuclear magnetic resonance (NMR) spectra, where peaks of hydrogen from alkene conjugated to the ketone of chalcone at δ 7.0–7.8 ppm disappeared and new aliphatic protons appeared in the expected region between δ 2.5 and 5.5 ppm as ABX spin system along with one –NH proton at δ 11.5 ppm. The two magnetically nonequivalent protons of the methylene group of the pyrazoline ring appeared distinctly at δ 2.5 and 3.5 ppm with *J* values ranging from 10 to 20 Hz. Additional peaks due to the alkyl, aryl, or acyl substitution on the pyrazoline ring confirmed the formation of the respective desired derivative. Representative derivatives were characterized by ¹³C NMR, and each spectrum showed the carbon values in the predictable regions. Also, every newly synthesized derivative was analyzed by high-resolution mass spectroscopy (HRMS) and the mass was confirmed with the calculated values of the target compounds.

2.2 | Biology activity

2.2.1 | In vitro antimicrobial activity

The antimicrobial activity evaluation of all pyrazoline derivatives was performed at The Community for Antimicrobial Drug Discovery (CO-ADD),^[33] funded by the Wellcome Trust (UK) and The University of Queensland (Australia). The screening was done at 32 μ g/ml against five

bacterial strains, Gram-positive *Staphylococcus aureus* and Gram-negative *Escherichia coli*, *Klebsiella pneumoniae*, *Acinetobacter baumannii*, and *Pseudomonas aeruginosa* using ciprofloxacin as a positive control. At the same concentration, the antifungal activity was also tested against two fungal species, that is, *Candida albicans* and *Cryptococcus neoformans* var. *grubii*, using fluconazole as a positive control. The obtained in vitro assay results are described as % growth inhibition (GI) in Table 1. This preliminary in vitro antimicrobial evaluation revealed that ~50% GI was displayed by compounds **14c**, **14f**, and **14i** against *A. baumannii* and compound **15o** against *C. albicans*.

2.2.2 | SAR exploration as an antibacterial study

From the obtained results, it was observed that all acid compounds showed a significant activity against Gram-negative *A. baumannii* and each structurally comparable hydrazine derivative also displayed equivalent results. The % GI was found to be increased by the introduction of groups into each chalcone-acid derivative in the following order: 4-chlorophenylhydrazine > phenylhydrazine > methylhydrazine. Notably, derivatives using 4-chlorophenylhydrazine, that is, **14c**, **14f**, and **14i**, exhibited GI >50% at 32 μ g/ml concentration, whereas compound **14c** revealed the highest activity, 56.60%, against Gram-negative *A. baumannii*. Hence, based on the structure–activity relationships, it can

TABLE 1 In vitro antimicrobial activities (% growth inhibition) of tested compounds at 32 µg/ml

Compound	<i>Staphylococcus aureus</i>	<i>Escherichia coli</i>	<i>Klebsiella pneumoniae</i>	<i>Pseudomonas aeruginosa</i>	<i>Acinetobacter baumannii</i>	<i>Candida albicans</i>	<i>Cryptococcus neoformans</i> var. <i>grubii</i>
14a	-	-	11.3	15.1	13.2	-	-
14b	-	-	23.9	-	48.1	10.6	-
14c	-	-	-	-	56.6	-	-
14d	-	-	-	-	10.4	-	-
14e	-	-	17.3	-	37.5	-	-
14f	-	-	35.6	-	50.9	-	-
14g	35.6	-	14.0	-	-	-	-
14h	13.8	-	13.8	11.1	12.3	-	-
14i	-	-	18.7	-	51.1	-	-
15a	13.5	-	12.6	14.1	19.6	-	-
15b	14.1	-	-	15.5	17.0	-	-
15c	15.9	-	-	10.3	13.8	-	-
15d	19.0	-	12.1	17.5	20.2	-	-
15e	21.5	-	-	-	26.3	-	-
15f	20.7	-	14.4	14.1	11.7	-	-
15g	10.9	-	33.6	18.1	34.4	-	-
15h	-	-	26.0	10.2	19.2	14.4	-
15i	17.0	-	16.8	15.3	13.3	17.0	-
15j	11.1	-	17.7	10.8	23.5	-	-
15k	-	-	25.5	-	40.2	12.1	-
15l	12.9	-	-	-	14.3	21.3	-
15m	12.5	-	-	17.1	15.7	-	-
15n	-	-	-	11.7	14.5	10.1	-
15o	13.8	-	-	10.4	12.7	55.7	-

Note: “-” not active (% GI < 10). Bold faced numerical values highlight the most potent compounds.

be concluded that, in the case of acid derivatives, the electron-donating group on the aromatic ring and, in contrast, the electron-withdrawing group on phenylhydrazine would result in a more potent compound as an antibacterial agent. None of the acid derivatives showed any potency against both fungal species.

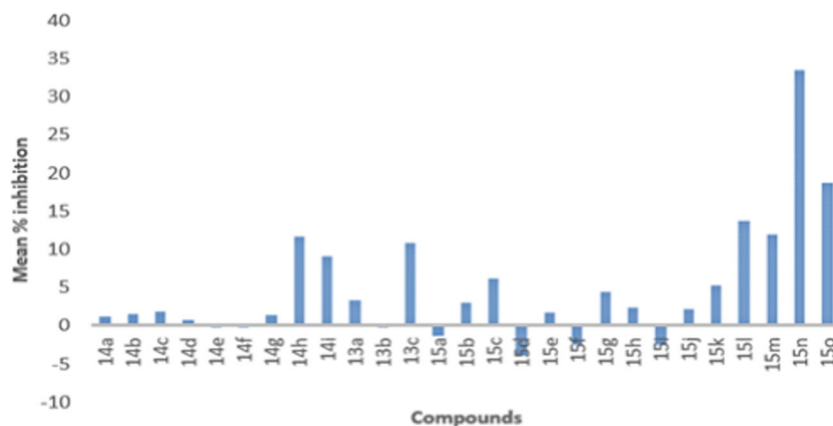
2.2.3 | In vitro antiproliferative activity

All the structures of novel derivatives were submitted to the National Cancer Institute (NCI) and further selected by the Developmental Therapeutics Program (www.dtp.nci.nih.gov) for in vitro anticancer screening. As per standard protocol of NCI, all compounds were evaluated for their antiproliferative activity at single-dose assay (10 µM concentration in dimethyl sulfoxide [DMSO]) on a panel of 60 cancer cell lines derived from leukemia, non-small-cell lung, colon, central nervous system (CNS), melanoma, ovarian, renal, prostate, and breast cancer as per protocol. The mean percentage inhibition of each tested compound

against the NCI-60 cell lines is calculated by dividing the summation of % GI values over the number of tested cell lines and is illustrated in Figure 2. This summarized data revealed that compound **14h** from the acid series and compound **15n** from amide series were the most potent derivatives.

The % GI values were calculated from percent of growth of the treated cells that were determined in comparison to the untreated control cells,^[34–37] and conclusive results of each tested compound are presented in Tables 2 and 3. Among all the nine acid derivatives, five derivatives, **14b**, **14c**, **14f**, **14g**, and **14h**, showed >50% GI against the A498 cell line from renal cancer even at such a small dose. Notably, all acid compounds displayed the maximum sensitivity against the A498 cell line from renal cancer, whereas the most significant compound, 5-(1,3-diphenyl-4,5-dihydro-1H-pyrazol-5-yl)-2,4-dimethyl-1H-pyrrole-3-carboxylic acid **14b**, displayed 70.2% GI. Among the amide derivatives, most active compound 5-(1-acetyl-3-(3-fluoro-4-(trifluoromethyl)phenyl)-4,5-dihydro-1H-pyrazol-5-yl)-2,4-dimethyl-N-(2,2,2-trifluoroethyl)-1H-pyrrole-3-carboxamide **15n** displayed a significant anticancer activity

FIGURE 2 Mean percentage inhibition values of all compounds against the NCI-60 cell line panel at 10 μ M concentration



against almost all cancer cell lines, with few exceptions. It displayed the highest efficiency against the SNB-75 cell line from CNS cancer with 8.37% cytotoxicity along with 100% GI (Table 4). Also, most of the amide compounds were highly sensitive against the A498 cell line from renal cancer. Hence from the obtained results, it can be concluded that compounds **14b** and **15n** exhibited a significant anticancer potency equivalent to that of sunitinib (A498, IC_{50} : 5.2 μ M; SNB-75, IC_{50} : 5.3 μ M; source: NCI database).

2.2.4 | SAR exploration as an antiproliferative study of acid derivatives 14a-i

The structural comparison concerning mean percentage inhibitions reveals that all amide derivatives demonstrated higher inhibition than the corresponding acid compounds. In both

cases of acid and amide derivatives, compounds comprising 3-fluoro-4-trifluoromethylphenyl ring were more potent than the related phenyl and thiophene derivatives. In detail, the structure-reactivity relationship of tested compounds for leukemia, colon, and CNS cancer cell lines reveals that, for the aromatic substituent, 3-fluoro-4-trifluoromethyl ring (compounds **14g-i**) was more favorable than the phenyl and thiophene ring (compounds **14a-f**), whereas 4-chlorophenyl and phenylpyrazoline rings (compounds **14h** and **14i**) were more significant than the methyl pyrazoline moiety (compound **14g**). Contradictorily, phenyl ring derivatives **14a-c** were more active against the A498 cell line from renal cancer than the compounds with thiophene and 3-fluoro-4-trifluoromethyl rings (compounds **14d-i**); however, the introduction of phenyl and 4-chlorophenylpyrazoline moieties leads to the most active compounds **14b** and **14c** with 70.20% and 60.72% GI, respectively.

TABLE 2 In vitro anticancer activities of tested acid derivatives at a concentration of 10 μ M^a

Compound	NSC No.	% Growth inhibition (GI)							
		Leukemia cancer		Colon cancer	CNS cancer		Renal cancer	Breast cancer	
		RPMI-8226	MOLT-4	HCT-15	SF-268	SNB-75	A498	UO-31	MCF7
14a	821320	-	-	-	-	14.22	45.26	16.34	-
14b	821319	-	-	-	-	13.14	70.20	11.03	11.92
14c	821321	-	-	-	-	14.74	60.72	11.26	17.73
14d	821328	-	-	-	-	-	-	20.22	-
14e	821322	-	-	10.44	-	-	45.99	10.70	18.32
14f	821329	-	-	-	-	11.76	57.36	17.09	-
14g	821326	-	-	-	-	-	53.42	12.00	-
14h	821325	31.36	23.26	24.38	18.63	22.57	57.16	27.74	32.14
14i	821327	35.74	23.80	25.43	20.53	27.59	32.51	28.18	35.62

Note: "-" not active (% GI < 10). Bold faced numerical values highlight the most potent compounds. Abbreviation: CNS, central nervous system.

^aSupporting Information includes growth percentage data for each NCI-60 cell line.

TABLE 3 In vitro anticancer activities of tested amide derivatives at a concentration of 10 μM ^a

Compound	NSC No.	% Growth inhibition (GI)								
		Leukemia cancer			Non-small-cell lung cancer A549/ATCC	CNS cancer SF-295	Renal cancer			Breast cancer MCF7
		MOLT-4	RPMI-8226	A498			CAKI-1	RXF 393	UO-31	
13a	821323	-	-	-	-	35.86	14.33	21.77	12.62	13.64
13b	821324	-	-	-	-	18.97	13.26	24.27	-	10.77
13c	819928	26.10	37.93	16.90	18.85	23.81	16.76	15.81	27.72	21.81
15a	821331	-	-	-	-	-	-	21.20	17.37	10.93
15b	821330	23.79	-	-	-	53.20	19.85	28.80	25.33	20.50
15c	821332	28.79	16.39	11.32	-	20.21	26.88	17.77	26.92	29.52
15d	821333	-	-	-	-	39.18	-	-	13.46	14.91
15e	821334	-	-	-	-	48.68	14.53	25.93	17.92	-
15f	821336	-	-	-	-	-	-	-	14.65	-
15g	821335	19.31	11.20	-	-	79.06	23.59	25.45	28.84	16.31
15h	821337	11.62	-	-	-	39.51	20.80	22.83	22.77	10.01
15i	821338	-	-	-	-	46.75	-	-	13.14	12.32
15j	821339	-	-	-	-	29.11	14.10	16.86	25.13	-
15k	821341	27.13	-	-	-	69.21	18.90	-	28.03	19.35
15l	821340	41.67	29.34	15.22	12.86	51.81	41.04	19.23	41.23	43.47
15m	821342	31.97	22.02	21.41	-	25.34	14.86	15.92	39.77	32.13
15n	821343	17.41	-	44.25	29.12	45.07	41.26	69.05	73.97	26.40
15o	821344	16.55	12.17	40.36	50.76	26.40	33.77	42.07	-	17.79

Note: “-” not active (% GI < 10). Bold faced numerical values highlight the most potent compounds.

Abbreviation: CNS, central nervous system.

^aSupporting Information includes growth percentage data for each NCI-60 cell line.

2.2.5 | SAR exploration as an antiproliferative study of amide derivatives 15a–o

Structural examination of all compounds with respect to the antiproliferative activity showed that almost all the pyrazoline compounds were more potent than the parent chalcone derivatives (compounds **13a–c**). In the case of phenyl and thiophene rings, phenylpyrazoline derivatives (compounds **15b** and **15g**) and 4-chlorophenylpyrazoline derivatives (compounds **15c** and **15h**) displayed higher potency than the rest of pyrazoline derivatives, whereas the carbonyl hydrazine derivatization led to the less

active compounds. There was no selective difference between the phenyl and thiophene derivatives, but 3-fluoro-4-trifluorophenyl ring was favorable to boost activity against almost all cancer cell lines. Within the 3-fluoro-4-trifluorophenyl derivatives, acetyl pyrazoline derivative **15n** was the most potent compound against almost all cancer cell lines and displayed the highest 100% GI with 8.37% cytotoxicity for SNB-75 cell line from CNS cancer. Hence, the SAR for anticancer activity can be concluded as the electron-withdrawing group on the aromatic ring and carbonyl substitution on the pyrazoline ring would deliver a more potent compound as an anticancer agent.

TABLE 4 In vitro anticancer activities of compound **15n** at a concentration of 10 μM

% Growth inhibition (GI)													
Colon cancer HCT-116	CNS cancer		Melanoma cancer MALME-3M	Ovarian cancer		Renal cancer			Breast cancer				
	SNB-19	SNB-75		OVCAR-4	OVCAR-8	786-0	ACHN	RXF 393	SN12C	UO-31	MDA-MB-231	HS 578T	T-47D
65.98	52.13	108.37	56.53	86.44	58.13	86.94	81.31	69.05	49.94	73.97	61.17	68.19	56.50

TABLE 5 Calculated rule-of-five parameters by SwissADME

Compound	mlogP	Number of H bond donors	Number of H bond acceptors	Molecular weight	C druglikeness
14b	3.14	2	3	359.42	Yes
14c	3.65	2	3	393.87	Yes
14f	3.25	2	3	399.89	Yes
14g	3.22	2	7	383.34	Yes
14h	4.33	2	7	445.41	Yes
15b	3.50	2	5	440.46	Yes
15c	3.97	2	5	474.91	Yes
15g	3.12	2	5	446.49	Yes
15k	3.57	2	9	464.38	Yes
15l	4.63	2	9	526.45	No
15n	3.30	2	10	492.39	Yes
15o	3.91	2	10	532.45	No

2.2.6 | Cytotoxicity and hemolysis

The toxicity study was performed at CO-ADD, Australia.^[33] The study was carried out on two random representative potent compounds **14c** and **14f** for their in vitro cytotoxic activity against human embryonic kidney (HEK293) cell line, which demonstrated that both tested compounds possessed no toxic effect ($CC_{50} > 80 \mu\text{M}$). Furthermore, the hemolysis assay of the same derivatives displayed HC_{10}/HC_{50} values $> 80 \mu\text{M}$ and confirmed the nontoxic property of the tested compounds against human red blood cells.

2.3 | In silico study

2.3.1 | Prediction of druglikeness by Lipinski's rule of five (RO5)

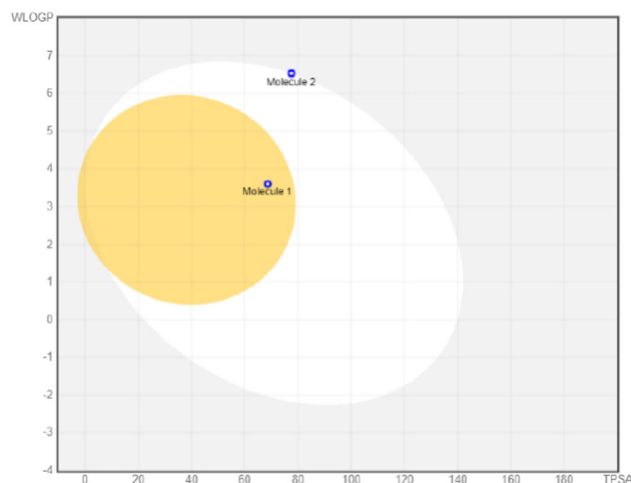
Lipinski's RO5^[38] ($MW \leq 500$, $mlogP \leq 4.15$, N or O ≤ 10 , NH, or OH ≤ 5) is the well-known thumb rule to predict the druglikeness properties of biologically potent compounds. Hence, RO5 parameters of the most potent derivatives were assessed by the SwissADME (<http://www.swissadme.ch/>). The calculated values (Table 5) approved that all the potent derivatives obeyed the RO5 and presented the significant druglikeness values, except **15l** and **15o**, which violated only the molecular weight parameter.

2.3.2 | ADME prediction

In silico ADME parameters and pharmacokinetic profile of compounds **14b** and **15n** were assessed by the freely offered web server SwissADME (<http://www.swissadme.ch/>). The obtained results in the form of figures are provided in Supporting Information that revealed the substantial ADME properties of studied derivatives. Compounds

14b and **15n** exhibited a good lipophilic property with consensus $\log P_{o/w}$ value of 3.64 and 4.62, respectively, together with moderate water solubility and high gastrointestinal absorption. The pink area of the bioavailability radar chart has signified the advantageous values of saturation (INSATU), size (SIZE), polarity (POLAR), solubility (INSOLU), lipophilicity (LIPO), and flexibility (FLEX) about oral bioavailability.^[39,40] Thus, compound **15n** is absolutely under the pink area, which signifies its good predicted oral bioavailability, whereas compound **14b** is found to be slightly deviating from the required solubility value, which could be rectified in the further derivatization.

The BOILED-Egg graph (Figure 3) identifies that compounds **14b** and **15n** were predicted to be effluated from the CNS by the P-glycoprotein, which clearly reduced the possibility of their resistance by tumor cell lines through efflux. Compound **14b** (molecule 1 in Figure 3) is predicted to passively permeate through the blood-brain barrier, whereas compound

**FIGURE 3** BOILED-Egg graph of compounds **14b** and **15n** from SwissADME web server

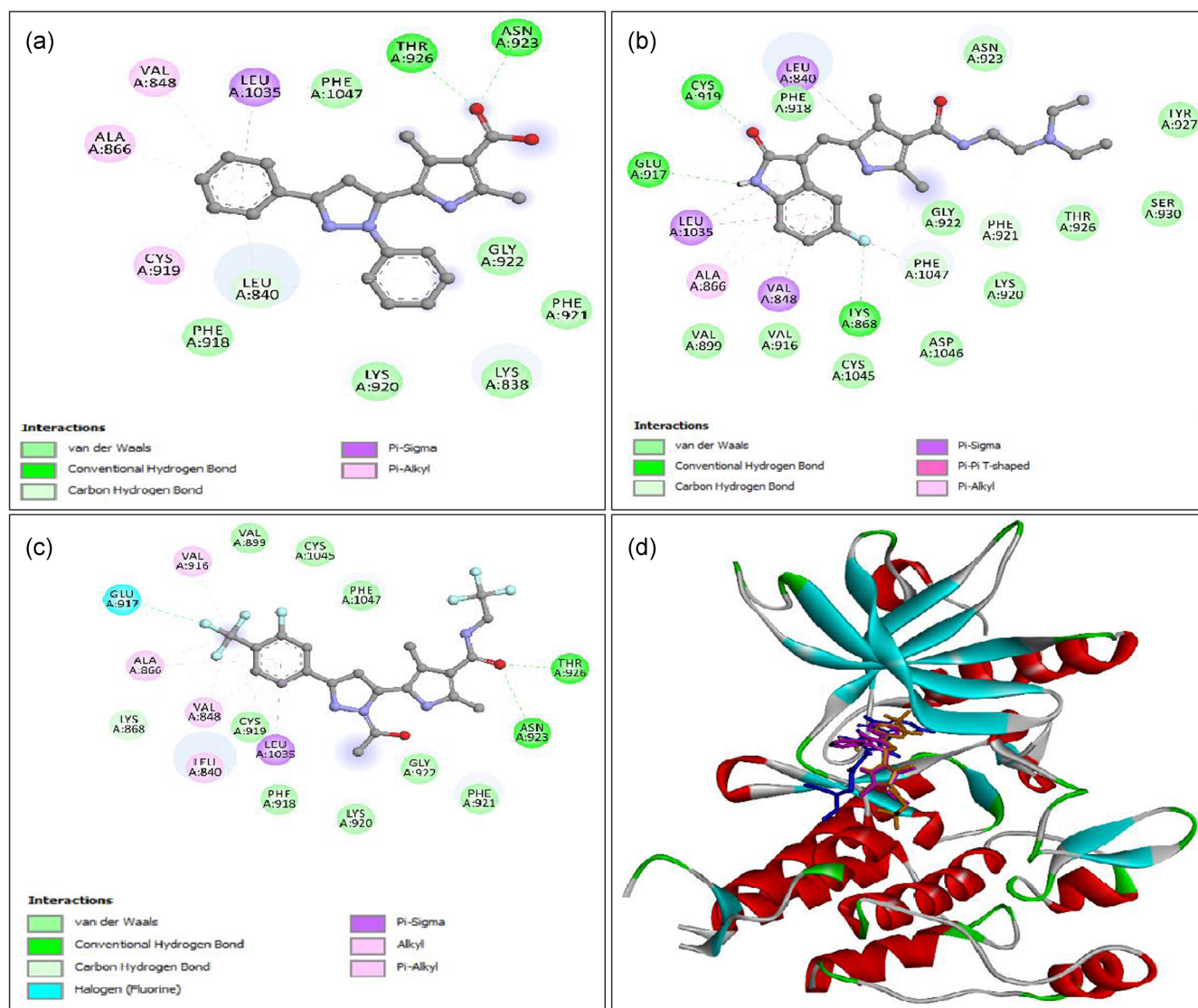


FIGURE 4 Docking images of compounds **14b** and **15n** and sunitinib. (a) A 2D diagram of bonding interaction between compound **14b** and VEGFR-2. (b) A 2D diagram of bonding interaction between sunitinib and VEGFR-2. (c) A 2D diagram of bonding interaction between compound **15n** and VEGFR-2. (d) Alignment of sunitinib (carbons are colored as blue), compound **14b** (carbons are colored as purple), and **15n** (carbons are colored as brown) in the active adenosine triphosphate site of protein

15n (molecule 2 in Figure 3) is predicted to be passively absorbed by the gastrointestinal tract.^[41] Overall, compounds **14b** and **15n** have promising in vitro anticancer activity along with the essential in silico ADME properties for druglikeness, hence signifying that both derivatives would be noble drug candidates.

2.3.3 | Molecular docking study

Molecular docking is an effective and reliable tool to understand the plausible orientation along with binding affinity between ligand and target protein, which induces the biological behavior of drug molecules. The drug candidate sunitinib displays the anticancer activity via inhibition of receptor tyrosine kinases like VEGFR-2.^[42] Hence, a

molecular docking study was performed using the most potent derivatives **14b** and **15n** at the active adenosine triphosphate (ATP)-binding site of VEGFR-2 with PDB ID: 4AGD (resolution: 2.81 Å) along with sunitinib. Results revealed that compounds **14b** and **15n** along with sunitinib as a co-crystallized ligand inside the active ATP-binding site of VEGFR-2 adopted a similar molecular orientation, which might be responsible for the observed affinity of the compounds **14b** and **15n** (Figure 4).

Sunitinib displayed a strong binding interaction between (2-oxindolin-3-ylidene)methylpyrrole moiety and ATP-binding site of VEGFR-2 through three hydrogen bonds at Glu917, Cys919, and Lys868. In the case of compound **14b**, oxygen of the carbonyl group acted as an H-acceptor and formed two conventional hydrogen bonding with the Thr926 and Asn923 with distances 1.92 and 2.43 Å,

respectively. The phenyl and pyrazoline rings get accommodated in the hydrophobic pocket made of Leu840, Val848, Ala866, and Cys919. The binding pose of **14b** was stabilized through exposure to the wide network of favorable van der Waals interactions with Phe1047, Phe918, Lys920, Lys838, Phe921, and Gly922. Similar to **14b**, carbonyl oxygen of compound **15n** acted as an H-acceptor, resulting in the formation of two conventional hydrogen bonds with Thr926 and Asn923 with distances 1.97 and 2.34 Å, respectively. The substituted phenyl and pyrazoline rings were overlapped by the hydrophobic pocket consisting of Leu1035, Val848, Ala866, Val916, and Leu840. The binding pose of **15n** was stabilized through exposure to the wide network of favorable van der Waals interactions with Val899, Cys1045, Phe1047, Cys919, Phe918, Lys920, and Gly922. The docking study for the best-scored conformations exhibited a binding affinity for compound **14b** (−7.9 kcal/mol) and **15n** (−9.5 kcal/mol), which was comparable with the ligand sunitinib (−9.9 kcal/mol). Hence, the described docking score data suggested that the potent derivatives **14b** and **15n** have good potential to inhibit VEGFR-2 as well as clarified the experimental anticancer results.

3 | CONCLUSION

This study offered a bunch of potent compounds against various microbial strains and cancer cell lines like **14f** (50.87% GI), **14c** (56.60% GI), and **14i** (51.14% GI) against Gram-negative *A. baumannii*, **15o** (55.74% GI) against fungal strain *C. albicans* at 32 µg/ml, as well as **14b** (70.20% GI), **14c** (60.72% GI), **14f** (57.36% GI), **14g** (53.42% GI), **14h** (57.16% GI), **15b** (53.20% GI), **15c** (50.21% GI), **15g** (79.06% GI), **15k** (69.21% GI), and **15l** (51.81% GI) against A498 cell line from renal cancer and **15o** (50.76% GI) against SF-295 from CNS cancer at 10 µM concentration. Among all acid and amide derivatives, compound **15n** is the most active compound against numerous cancer cell lines and it displayed 100.0% GI with 8.37% cytotoxicity for SNB-75 cell line from CNS cancer. Overall, the antiproliferative assay of all newly demonstrated pyrazoline-pyrrole derivatives revealed that the several compounds exhibited anticancer potency analogous to sunitinib (IC₅₀: 4.0–8.0 µM). SAR study revealed that the dramatic improvement in the bioactivity of the amide derivatives may be due to the conjugative effect of the electron-withdrawing group on the aryl ring, that is, trifluoromethyl at *para*-position and carbonyl pyrazoline. In vitro toxicity study of the representative potent compounds signified a potential for a good therapeutic index. In silico ADME study of most active compounds, **14b** and **15n**, comply with the desired ADME parameters and also obey Lipinski's rule of five for druglikeness. The molecular docking study concluded that the tighter interactions of **14b** and **15n** at the active ATP site of VEGFR-2 might be responsible for anticancer potency. Hence, the proposed pyrazoline-pyrrole template can be a potential scaffold to develop the new multitargeted anticancer drug as well as antimicrobial drugs, and additionally, compounds **14b** and **15n** would be noble drug candidates for the clinical treatment of numerous cancers.

4 | EXPERIMENTAL

4.1 | Chemistry

4.1.1 | General

All the reagents and solvents were procured from Spectrochem, Sigma-Aldrich, S D Fine-Chem, and Finar Chemicals and used without any further purification. The progress of reactions was monitored by analytical thin-layer chromatography (TLC; silica gel 60 F₂₅₄ plates from Merck, Darmstadt, Germany). The TLC plates were visualized under short- and long-wavelength UV light. Melting points were uncorrected and confirmed in an open capillary tube. HRMS spectra were recorded on a Waters SYNAPT G2 HDMS system with triple quadrupole mass spectrometer (ESI mode) and the values were expressed in units of *m/z*. All the ¹H and ¹³C NMR spectra were recorded in DMSO-*d*₆ on a Bruker Avance-III 500 MHz spectrometer using tetramethylsilane as an internal solvent. Chemical shift and coupling constant values were expressed in ppm and Hz, respectively. The abbreviations used to describe the peak patterns are singlet (s), doublet (d), triplet (t), multiplet (m), double doublet (dd), and so on. All the compounds, **12a–c** and **13a–c**, were synthesized as per the reported procedure.^[30]

The InChI codes of the investigated compounds, together with some biological activity data, are provided as Supporting Information.

4.1.2 | General procedure for the synthesis of compounds **14a–i**, **15a–c**, **15f–h**, **15k–m**

To a solution of chalcone derivative (1.0 g, 1.0 equiv) in ethanol (25 ml, 5.0 volumes), hydrazine derivative (1.5 equiv) and NaOH (2.0 equiv) were added at 20–25°C. The mixture was refluxed for 2 hr and the progress of the reaction was monitored by TLC. After the complete conversion, the mixture was poured over an ice–water mixture (50 ml, 50.0 volumes). For acid derivatives, the mass was acidified to pH ~5 with acetic acid. The precipitate was filtered and washed with water under vacuum. The solid product was dried under vacuum and purified in ethyl *tert*-butyl ether (MTBE) by the method of trituration.

4.1.3 | General procedure for the synthesis of compounds **15d**, **15e**, **15i**, **15j**, **15n**, and **15o**

To a solution of chalcone derivative (1.0 g, 1.0 equiv) in ethanol (10 ml, 10.0 volumes), 99% hydrazine hydrate (2.0 volumes) was added, and the mixture was refluxed for 2 hr. The progress of the reaction was monitored by TLC. After the complete conversion, the mixture was poured over an ice–water mixture (50 ml, 50.0 volumes) and it was extracted with chloroform (2 × 5.0 volumes) twice. The organic layer was washed with brine solution (5 ml, 5 volumes) and dried over sodium sulfate. The dried organic layer was cooled at ~10°C and was charged with triethylamine (2.5 equiv), followed by

carbonyl chloride derivative (1.1 equiv). The mixture was stirred at room temperature for 2 hr and the progress of the reaction was monitored by TLC. After the complete conversion, the mixture was poured over an ice-water mixture (50 ml, 50.0 volumes). The organic layer was separated and concentrated till slurry mass. Hexane (5 ml, 5.0 volumes) was added and the precipitate was filtered. The solid product was dried under vacuum to get the pure compound.

2,4-Dimethyl-5-(1-methyl-3-phenyl-4,5-dihydro-1H-pyrazol-5-yl)-1H-pyrrole-3-carboxylic acid (14a)

The product was obtained as an off-white solid; yield: 0.41 g, 74.3%; R_F (mobile phase hexanes/EtOAc 50:50): 0.45; m.p.: 171–173°C; ^1H NMR (500 MHz, DMSO- d_6): δ 11.49 (br s, 1H, -COOH), 11.08 (s, 1H, -NH), 7.64 (d, J = 9.0 Hz, 2H, Ar-H), 7.37 (m, 3H, Ar-H), 4.15 (dd, J = 18.5, 12.5 Hz, 1H, -CH $_X$), 3.36 (t, J = 12.5 Hz, 1H, -CH $_A$ H), 3.02 (t, J = 19.5 Hz, 1H, -CH $_B$ H), 2.66 (s, 3H, -NCH $_3$), 2.36 (s, 3H, pyrrole -CH $_3$), 2.14 (s, 3H, pyrrole -CH $_3$); HRMS (ESI) calcd. for $[\text{M}+\text{H}]^+$ $\text{C}_{17}\text{H}_{20}\text{N}_3\text{O}_2$: 298.1555, found: 298.1554.

5-(1,3-Diphenyl-4,5-dihydro-1H-pyrazol-5-yl)-2,4-dimethyl-1H-pyrrole-3-carboxylic acid (14b)

The product was obtained as an off-white solid; yield: 0.52 g, 77.9%; R_F (mobile phase hexanes/EtOAc 50:50): 0.70; m.p.: 195–197°C; ^1H NMR (500 MHz, DMSO- d_6): δ 11.53 (br s, 1H, -COOH), 11.06 (s, 1H, -NH), 7.76 (d, J = 9.5 Hz, 1H, Ar-H), 7.44 (t, J = 8.5 Hz, 2H, Ar-H), 7.38 (t, J = 9.0 Hz, 1H, Ar-H), 7.18 (t, J = 10.0 Hz, 1H, Ar-H), 7.03 (d, J = 10.0 Hz, 1H, Ar-H), 7.75 (t, J = 9.0 Hz, 1H, Ar-H), 5.30 (dd, J = 15.0, 12.5 Hz, 1H, -CH $_X$), 3.80 (dd, J = 22.0, 15.5 Hz, 1H, -CH $_A$ H), 3.11 (dd, J = 22.0, 12.0 Hz, 1H, -CH $_B$ H), 2.30 (s, 3H, pyrrole -CH $_3$), 2.21 (s, 3H, pyrrole -CH $_3$); ^{13}C NMR (126 MHz, DMSO- d_6): δ 145.76, 143.85, 133.69, 130.85, 127.15, 126.98, 124.17, 124.01, 117.38, 114.86, 111.54, 54.78, 39.12, 37.85, 11.80, 9.16; HRMS (ESI) calcd. for $[\text{M}+\text{H}]^+$ $\text{C}_{22}\text{H}_{22}\text{N}_3\text{O}_2$: 360.1712, found: 360.1713.

5-[1-(4-Chlorophenyl)-3-phenyl-4,5-dihydro-1H-pyrazol-5-yl]-2,4-dimethyl-1H-pyrrole-3-carboxylic acid (14c)

The product was obtained as off-white solid; yield: 0.61 g, 83.4%; R_F (mobile phase hexanes/EtOAc 50:50): 0.70; m.p.: 159–161°C; ^1H NMR (500 MHz, DMSO- d_6): δ 11.04 (s, 1H, -NH), 7.76 (d, J = 7.2 Hz, 2H, Ar-H), 7.42 (m, 3H, Ar-H), 7.22 (d, J = 8.9 Hz, 2H, Ar-H), 7.02 (d, J = 9.0 Hz, 2H, Ar-H), 5.32 (dd, J = 12.3, 9.6 Hz, 1H, -CH $_X$), 3.80 (dd, J = 17.4, 12.5 Hz, 1H, -CH $_A$ H), 3.14 (dd, J = 17.5, 9.4 Hz, 1H, -CH $_B$ H), 2.31 (s, 3H, pyrrole -CH $_3$), 2.20 (s, 3H, pyrrole -CH $_3$); ^{13}C NMR (126 MHz, DMSO- d_6): δ 148.65, 144.66, 135.60, 132.75, 129.30, 129.11, 129.06, 126.24, 125.67, 123.00, 117.18, 114.98, 56.84, 41.38, 13.91, 11.26; HRMS (ESI) calcd. for $[\text{M}+\text{H}]^+$ $\text{C}_{22}\text{H}_{21}\text{ClN}_3\text{O}_2$: 394.1322, found: 394.1309.

2,4-Dimethyl-5-[1-methyl-3-(thiophen-2-yl)-4,5-dihydro-1H-pyrazol-5-yl]-1H-pyrrole-3-carboxylic acid (14d)

The product was obtained as an off-white solid; yield: 0.42 g, 76.2%; R_F (mobile phase hexanes/EtOAc 50:50): 0.70; m.p.: 225–227°C; ^1H NMR (500 MHz, DMSO- d_6): δ 11.49 (br s, 1H, -COOH), 11.09 (s, 1H, -NH), 7.54 (dd, J = 5.1, 0.9 Hz, 1H, thiophene-H), 7.22 (dd, J = 3.5,

0.9 Hz, 1H, thiophene-H), 7.09 (dd, J = 5.0, 3.6 Hz, 1H, thiophene-H), 4.15 (dd, J = 15.0, 9.9 Hz, 1H, -CH $_X$), 3.33 (d, J = 10.0 Hz, 1H, -CH $_A$ H), 3.06 (t, J = 15.5 Hz, 1H, -CH $_B$ H), 2.62 (s, 3H, -NCH $_3$), 2.36 (s, 3H, pyrrole -CH $_3$), 2.14 (s, 3H, pyrrole -CH $_3$); HRMS (ESI) calcd. for $[\text{M}+\text{H}]^+$ $\text{C}_{15}\text{H}_{18}\text{N}_3\text{O}_2\text{S}^+$: 304.1119, found: 304.1117.

2,4-Dimethyl-5-[1-phenyl-3-(thiophen-2-yl)-4,5-dihydro-1H-pyrazol-5-yl]-1H-pyrrole-3-carboxylic acid (14e)

The product was obtained as a brown solid; yield: 0.52 g, 78.4%; R_F (mobile phase hexanes/EtOAc 40:60): 0.60; m.p.: 180–182°C; ^1H NMR (500 MHz, DMSO- d_6): δ 11.50 (br s, 1H, -COOH), 11.07 (s, 1H, -NH), 7.60 (d, J = 6.0 Hz, 1H, Ar-H), 7.27 (s, 1H, Ar-H), 7.15 (m, 3H, Ar-H), 6.96 (d, J = 10.0 Hz, 2H, Ar-H), 6.75 (t, J = 8.5 Hz, 1H, Ar-H), 5.29 (t, J = 13.0 Hz, 1H, -CH $_X$), 3.79 (dd, J = 21.5, 16.0 Hz, 1H, -CH $_A$ H), 3.12 (dd, J = 21.5, 12.0 Hz, 1H, -CH $_B$ H), 2.30 (s, 3H, pyrrole -CH $_3$), 2.21 (s, 3H, pyrrole -CH $_3$); HRMS (ESI) calcd. for $[\text{M}+\text{H}]^+$ $\text{C}_{20}\text{H}_{20}\text{N}_3\text{O}_2\text{S}^+$: 366.1276, found: 366.1272.

5-[1-(4-Chlorophenyl)-3-(thiophen-2-yl)-4,5-dihydro-1H-pyrazol-5-yl]-2,4-dimethyl-1H-pyrrole-3-carboxylic acid (14f)

The product was obtained as an off-white solid; yield: 0.58 g, 79.9%; R_F (mobile phase hexanes/EtOAc 50:50): 0.60; m.p.: 189–191°C; ^1H NMR (500 MHz, DMSO- d_6): δ 11.54 (br s, 1H, -COOH), 11.09 (s, 1H, -NH), 7.62 (d, J = 6.0 Hz, 1H, thiophene-H), 7.29 (d, 1H, J = 4.0 Hz, thiophene-H), 7.22 (d, J = 11.5 Hz, 2H, Ar-H), 7.12 (t, J = 5.5 Hz, 2H, thiophene-H), 6.93 (d, J = 13.7 Hz, 2H, Ar-H), 5.32 (dd, J = 15.0, 12.0 Hz, 1H, -CH $_X$), 3.81 (dd, J = 21.5, 15.5 Hz, 1H, -CH $_A$ H), 3.14 (dd, J = 21.5, 13.0 Hz, 1H, -CH $_B$ H), 2.29 (s, 3H, pyrrole -CH $_3$), 2.19 (s, 3H, pyrrole -CH $_3$); ^{13}C NMR (126 MHz, DMSO- d_6): δ 167.34, 145.16, 144.50, 136.20, 136.10, 129.11, 128.29, 128.13, 128.05, 125.64, 123.12, 117.32, 114.98, 110.81, 56.93, 42.17, 13.92, 11.21; HRMS (ESI) calcd. for $[\text{M}+\text{H}]^+$ $\text{C}_{20}\text{H}_{19}\text{ClN}_3\text{O}_2\text{S}^+$: 400.0886, found: 400.0872.

5-[3-[3-Fluoro-4-(trifluoromethyl)phenyl]-1-methyl-4,5-dihydro-1H-pyrazol-5-yl]-2,4-dimethyl-1H-pyrrole-3-carboxylic acid (14g)

The product was obtained as an off-white solid; yield: 0.44 g, 81.6%; R_F (mobile phase hexanes/EtOAc 50:50): 0.60; m.p.: 200–202°C; ^1H NMR (500 MHz, DMSO- d_6): δ 11.53 (br s, 1H, -COOH), 11.11 (s, 1H, -NH), 7.79 (t, J = 7.9 Hz, 1H, Ar-H), 7.64 (t, J = 9.9 Hz, 2H, Ar-H), 4.34 (dd, J = 14.9, 10.6 Hz, 1H, -CH $_X$), 3.41 (dd, J = 16.4, 10.5 Hz, 1H, -CH $_A$ H), 3.04 (t, J = 15.7 Hz, 1H, -CH $_B$ H), 2.72 (s, 3H, -NCH $_3$), 2.37 (s, 3H, pyrrole -CH $_3$), 2.15 (s, 3H, pyrrole -CH $_3$); ^{13}C NMR (126 MHz, DMSO- d_6): δ 167.36, 160.61, 158.60, 146.87, 140.24, 135.95, 128.10, 126.42, 124.27, 123.06, 122.11, 121.90, 119.95, 119.37, 113.51, 110.75, 63.91, 39.97, 38.77, 13.94, 11.17; HRMS (ESI) calcd. for $[\text{M}+\text{H}]^+$ $\text{C}_{18}\text{H}_{18}\text{F}_4\text{N}_3\text{O}_2$: 384.1335, found: 384.1334.

5-[3-[3-Fluoro-4-(trifluoromethyl)phenyl]-1-phenyl-4,5-dihydro-1H-pyrazol-5-yl]-2,4-dimethyl-1H-pyrrole-3-carboxylic acid (14h)

The product was obtained as an off-white solid; yield: 0.52 g, 83.0%; R_F (mobile phase hexanes/EtOAc 40:60): 0.70; m.p.: 127–129°C; ^1H NMR (500 MHz, DMSO- d_6): δ 11.54 (s, 1H, -COOH), 11.07 (s, 1H, -NH), 7.89–7.71 (m, 3H, Ar-H), 7.21 (t, J = 9.9 Hz, 2H, Ar-H), 7.09 (d,

$J = 10.0$ Hz, 2H, Ar-H), 6.81 (t, $J = 9.1$ Hz, 1H, Ar-H), 5.48 (dd, $J = 12.7$, 9.4 Hz, $-\text{CH}_X$), 3.80 (dd, $J = 17.6$, 13.0 Hz, 1H, $-\text{CH}_A\text{H}$), 3.16 (dd, $J = 17.6$, 9.3 Hz, 1H, $-\text{CH}_B\text{H}$), 2.30 (s, 3H, pyrrole $-\text{CH}_3$), 2.21 (s, 3H, pyrrole $-\text{CH}_3$); HRMS (ESI) calcd. for $[\text{M}+\text{H}]^+$ $\text{C}_{23}\text{H}_{20}\text{F}_4\text{N}_3\text{O}_2^+$: 446.1491, found: 446.1495.

5-[1-(4-Chlorophenyl)-3-[3-fluoro-4-(trifluoromethyl)phenyl]-4,5-dihydro-1H-pyrazol-5-yl]-2,4-dimethyl-1H-pyrrole-3-carboxylic acid (**14i**)

The product was obtained as an off-white solid; yield: 0.56 g, 82.9%; R_F (mobile phase hexanes/EtOAc 50:50): 0.70; m.p.: 151–153°C; ^1H NMR (500 MHz, DMSO- d_6): δ 11.56 (br s, 1H, $-\text{COOH}$), 11.07 (s, 1H, $-\text{NH}$), 7.80 (dt, $J = 24.9$, 8.1 Hz, 3H, Ar-H), 7.26 (d, $J = 8.9$ Hz, 2H, Ar-H), 7.06 (d, $J = 8.9$ Hz, 2H, Ar-H), 5.49 (dd, $J = 12.7$, 9.2 Hz, 1H, $-\text{CH}_X$), 3.82 (dd, $J = 17.7$, 13.0 Hz, 1H, $-\text{CH}_A\text{H}$), 3.18 (dd, $J = 17.6$, 9.0 Hz, 1H, $-\text{CH}_B\text{H}$), 2.30 (s, 3H, pyrrole $-\text{CH}_3$), 2.20 (s, 3H, pyrrole $-\text{CH}_3$); ^{13}C NMR (126 MHz, DMSO- d_6): δ 167.33, 160.63, 158.61, 146.03, 143.49, 139.76, 139.69, 136.24, 129.19, 128.11, 125.45, 124.27, 123.89, 122.27, 122.11, 117.61, 115.34, 114.03, 113.85, 110.87, 57.00, 40.72, 13.92, 11.20; HRMS (ESI) calcd. for $[\text{M}+\text{H}]^+$ $\text{C}_{23}\text{H}_{18}\text{ClF}_4\text{N}_3\text{O}_2^+$: 480.1102, found: 480.1093.

2,4-Dimethyl-5-(1-methyl-3-phenyl-4,5-dihydro-1H-pyrazol-5-yl)-N-(2,2,2-trifluoroethyl)-1H-pyrrole-3-carboxamide (**15a**)

The product was obtained as an off-white solid; yield: 0.45 g, 83.3%; R_F (mobile phase hexanes/EtOAc 50:50): 0.60; m.p.: 117–119°C; ^1H NMR (400 MHz, DMSO- d_6): δ 10.91 (s, 1H, $-\text{NH}$), 7.74 (t, 1H, $-\text{CONH}$), 7.64 (d, 2H, $J = 6.8$ Hz, Ar-H), 7.38 (t, $J = 6.8$ Hz, 2H, Ar-H), 7.33 (t, $J = 6.8$ Hz, 1H, Ar-H), 4.13 (m, $J = 10.0$ Hz, 1H, $-\text{CH}_X$), 4.00 (m, 2H, $-\text{NCH}_2$), 3.33 (m, 1H, $-\text{CH}_A\text{H}$), 3.01 (t, $J = 15.6$ Hz, 1H, $-\text{CH}_B\text{H}$), 2.66 (s, 1H, $-\text{NCH}_3$), 2.27 (s, 3H, pyrrole $-\text{CH}_3$), 2.07 (s, 3H, pyrrole $-\text{CH}_3$); HRMS (ESI) calcd. for $[\text{M}+\text{H}]^+$ $\text{C}_{19}\text{H}_{22}\text{F}_3\text{N}_4\text{O}^+$: 379.1745, found: 379.1749.

5-(1,3-Diphenyl-4,5-dihydro-1H-pyrazol-5-yl)-2,4-dimethyl-N-(2,2,2-trifluoroethyl)-1H-pyrrole-3-carboxamide (**15b**)

The product was obtained as an off-white solid; yield: 0.50 g, 79.5%; R_F (mobile phase hexanes/EtOAc 40:60): 0.70; m.p.: 227–229°C; ^1H NMR (500 MHz, DMSO- d_6): δ 10.91 (s, 1H, $-\text{NH}$), 7.76 (d, $J = 7.2$ Hz, 3H, $-\text{CONH}$), 7.44 (t, $J = 7.5$ Hz, 2H, Ar-H), 7.38 (t, $J = 7.1$ Hz, 1H, Ar-H), 7.18 (t, $J = 7.8$ Hz, 2H, Ar-H), 7.06 (d, $J = 8.0$ Hz, 2H, Ar-H), 6.76 (t, $J = 7.2$ Hz, 1H, Ar-H), 5.29 (dd, $J = 12.2$, 9.7 Hz, 1H, $-\text{CH}_X$), 4.08–3.87 (m, 2H, $-\text{NCH}_2$), 3.80 (dd, $J = 17.3$, 12.6 Hz, 1H, $-\text{CH}_A\text{H}$), 3.10 (dd, $J = 17.3$, 9.5 Hz, 1H, $-\text{CH}_B\text{H}$), 2.23 (s, 3H, pyrrole $-\text{CH}_3$), 2.14 (s, 3H, pyrrole $-\text{CH}_3$); ^{13}C NMR (126 MHz, DMSO- d_6): δ 166.67, 147.80, 145.91, 132.96, 130.58, 129.27, 129.10, 128.84, 126.62, 126.35, 126.12, 124.40, 122.18, 119.46, 115.47, 114.56, 113.65, 56.93, 41.35, 12.84, 10.38; HRMS (ESI) calcd. for $[\text{M}+\text{H}]^+$ $\text{C}_{24}\text{H}_{24}\text{F}_3\text{N}_4\text{O}^+$: 441.1902, found: 441.1897.

5-[1-(4-Chlorophenyl)-3-phenyl-4,5-dihydro-1H-pyrazol-5-yl]-2,4-dimethyl-N-(2,2,2-trifluoroethyl)-1H-pyrrole-3-carboxamide (**15c**)

The product was obtained as an off-white solid; yield: 0.53 g, 78.2%; R_F (mobile phase hexanes/EtOAc 50:50): 0.60; m.p.: 249–251°C; ^1H NMR (500 MHz, DMSO- d_6): δ 10.90 (s, 1H, $-\text{NH}$), 7.76 (d, $J = 7.1$ Hz, 3H, Ar-H, $-\text{CONH}$), 7.42 (dt, $J = 27.5$, 7.1 Hz, 3H, Ar-H), 7.23 (d,

$J = 8.4$ Hz, 2H, Ar-H), 7.03 (d, $J = 8.4$ Hz, 2H, Ar-H), 5.32 (t, $J = 10.5$ Hz, 1H, $-\text{CH}_X$), 4.07–3.89 (m, 2H, $-\text{NCH}_2$), 3.82 (dd, $J = 17.2$, 12.7 Hz, 1H, $-\text{CH}_A\text{H}$), 3.12 (dd, $J = 17.3$, 9.1 Hz, 1H, $-\text{CH}_B\text{H}$), 2.22 (s, 3H, pyrrole $-\text{CH}_3$), 2.13 (s, 3H, pyrrole $-\text{CH}_3$); ^{13}C NMR (126 MHz, DMSO- d_6): δ 166.61, 148.62, 144.59, 132.72, 130.73, 129.33, 129.12, 129.08, 126.61, 126.24, 125.87, 124.39, 122.99, 115.52, 114.98, 114.80, 56.82, 41.49, 12.83, 10.35; HRMS (ESI) calcd. for $[\text{M}+\text{H}]^+$ $\text{C}_{24}\text{H}_{23}\text{ClF}_3\text{N}_4\text{O}^+$: 475.1512, found: 475.1504.

5-(1-Acetyl-3-phenyl-4,5-dihydro-1H-pyrazol-5-yl)-2,4-dimethyl-N-(2,2,2-trifluoroethyl)-1H-pyrrole-3-carboxamide (**15d**)

The product was obtained as an off-white solid; yield: 0.48 g, 82.8%; R_F (mobile phase hexanes/EtOAc 50:50): 0.25; m.p.: 280–282°C; ^1H NMR (500 MHz, DMSO- d_6): δ 10.73 (s, 1H, $-\text{NH}$), 7.88–7.67 (m, 3H, Ar-H, $-\text{CONH}$), 7.48 (d, $J = 3.4$ Hz, 3H, Ar-H), 5.47 (dd, $J = 6.0$ Hz, 1H, $-\text{CH}_X$), 4.05–3.87 (m, 2H, $-\text{NCH}_2$), 3.78 (dd, $J = 18.0$, 12.6 Hz, 1H, $-\text{CH}_A\text{H}$), 3.15 (dd, $J = 18.2$, 6.0 Hz, 1H, $-\text{CH}_B\text{H}$), 2.23 (d, $J = 8.5$ Hz, 6H, $-\text{NCOCH}_3$, pyrrole $-\text{CH}_3$), 2.03 (s, 3H, pyrrole $-\text{CH}_3$); HRMS (ESI) calcd. for $[\text{M}+\text{H}]^+$ $\text{C}_{20}\text{H}_{22}\text{F}_3\text{N}_4\text{O}_2^+$: 407.1695, found: 407.1696.

5-[1-(Cyclobutanecarbonyl)-3-phenyl-4,5-dihydro-1H-pyrazol-5-yl]-2,4-dimethyl-N-(2,2,2-trifluoroethyl)-1H-pyrrole-3-carboxamide (**15e**)

The product was obtained as an off-white solid; yield: 0.54 g, 84.7%; R_F (mobile phase hexanes/EtOAc 50:50): 0.50; m.p.: 259–261°C; ^1H NMR (500 MHz, DMSO- d_6): δ 10.75 (s, 1H, $-\text{NH}$), 7.82–7.75 (m, 2H, Ar-H), 7.73 (t, $J = 6.2$ Hz, 1H, $-\text{CONH}$), 7.47 (d, $J = 4.8$ Hz, 3H, Ar-H), 5.44 (dd, $J = 12.4$, 6.3 Hz, 1H, $-\text{CH}_X$), 4.06–3.87 (m, 2H, $-\text{NCH}_2$), 3.76 (m, 2H, $-\text{COCH}$, $-\text{CH}_A\text{H}$), 3.12 (dd, $J = 18.1$, 6.3 Hz, 1H, $-\text{CH}_B\text{H}$), 2.22 (s, 3H, pyrrole $-\text{CH}_3$), 2.14 (m, 4H, $-\text{CH}_2\text{H}(\text{CH}_2)\text{CH}_2\text{H}$), 2.03 (s, 3H, pyrrole $-\text{CH}_3$), 1.95 (dq, $J = 18.3$, 9.3 Hz, 1H, $-\text{COCCH}_2\text{H}$), 1.74 (dt, $J = 16.2$, 8.0 Hz, 1H, $-\text{COCCH}_2\text{H}$); HRMS (ESI) calcd. for $[\text{M}+\text{H}]^+$ $\text{C}_{23}\text{H}_{26}\text{F}_3\text{N}_4\text{O}_2^+$: 447.2008, found: 447.0765.

2,4-Dimethyl-5-[1-methyl-3-(thiophen-2-yl)-4,5-dihydro-1H-pyrazol-5-yl]-N-(2,2,2-trifluoroethyl)-1H-pyrrole-3-carboxamide (**15f**)

The product was obtained as an off-white solid; yield: 0.45 g, 83.4%; R_F (mobile phase hexanes/EtOAc 50:50): 0.50; m.p.: 177–179°C; ^1H NMR (500 MHz, DMSO- d_6): δ 10.92 (s, 1H, $-\text{NH}$), 7.75 (t, $J = 6.4$ Hz, 1H, $-\text{CONH}$), 7.54 (d, $J = 4.5$ Hz, 1H, thiophene-H), 7.22 (d, $J = 2.8$ Hz, 1H, thiophene-H), 7.09 (dd, $J = 4.9$, 3.7 Hz, 1H, thiophene-H), 4.13 (dd, $J = 14.9$, 9.9 Hz, 1H, $-\text{CH}_X$), 4.06–3.89 (m, 2H, $-\text{NCH}_2$), 3.31 (s, 1H, $-\text{CH}_A\text{H}$), 3.06 (dd, $J = 22.2$, 8.7 Hz, 1H, $-\text{CH}_B\text{H}$), 2.63 (s, 3H, $-\text{NCH}_3$), 2.28 (s, 3H, pyrrole $-\text{CH}_3$), 2.07 (s, 3H, pyrrole $-\text{CH}_3$); HRMS (ESI) calcd. for $[\text{M}+\text{H}]^+$ $\text{C}_{17}\text{H}_{20}\text{F}_3\text{N}_4\text{OS}^+$: 385.1310, found: 385.1309.

2,4-Dimethyl-5-[1-phenyl-3-(thiophen-2-yl)-4,5-dihydro-1H-pyrazol-5-yl]-N-(2,2,2-trifluoroethyl)-1H-pyrrole-3-carboxamide (**15g**)

The product was obtained as an off-white solid; yield: 0.49 g, 78.2%; R_F (mobile phase hexanes/EtOAc 50:50): 0.60; m.p.: 191–193°C; ^1H NMR (500 MHz, DMSO- d_6): δ 10.92 (s, 1H, $-\text{NH}$), 7.76 (t, $J = 6.3$ Hz, 1H, $-\text{CONH}$), 7.60 (d, $J = 5.0$ Hz, 1H, thiophene-H), 7.27 (d, $J = 3.3$ Hz,

1H, thiophene-H), 7.18 (t, $J = 7.5$ Hz, 2H, Ar-H), 7.12 (t, $J = 4.1$ Hz, 1H, thiophene-H), 6.99 (d, $J = 8.1$ Hz, 2H, Ar-H), 6.76 (t, $J = 7.2$ Hz, 1H, Ar-H), 5.28 (t, $J = 10.5$ Hz, 1H, $-\text{CH}_X$), 4.06–3.88 (m, 2H, $-\text{NCH}_2$), 3.80 (dd, $J = 17.1, 12.5$ Hz, 1H, $-\text{CH}_A\text{H}$), 3.10 (dd, $J = 17.2, 9.6$ Hz, 1H, $-\text{CH}_B\text{H}$), 2.23 (s, 3H, pyrrole $-\text{CH}_3$), 2.14 (s, 3H, pyrrole $-\text{CH}_3$); ^{13}C NMR (126 MHz, DMSO- d_6) δ 166.64, 145.77, 144.35, 136.40, 130.63, 129.29, 128.84, 128.24, 127.74, 127.71, 126.62, 126.06, 124.39, 122.17, 119.55, 115.46, 114.65, 113.67, 57.10, 42.15, 12.83, 10.36; HRMS (ESI) calcd. for $[\text{M}+\text{H}]^+$ $\text{C}_{22}\text{H}_{22}\text{F}_3\text{N}_4\text{O}_5^+$: 447.1466, found: 447.1470.

5-[1-(4-Chlorophenyl)-3-(thiophen-2-yl)-4,5-dihydro-1H-pyrazol-5-yl]-2,4-dimethyl-N-(2,2,2-trifluoroethyl)-1H-pyrrole-3-carboxamide (15h)

The product was obtained as an off-white solid; yield: 0.54 g, 80.0%; R_F (mobile phase hexanes/EtOAc 50:50): 0.75; m.p.: 227–229°C; ^1H NMR (500 MHz, DMSO- d_6): δ 10.92 (s, 1H, $-\text{NH}$), 7.76 (t, $J = 5.8$ Hz, 1H, $-\text{CONH}$), 7.63 (d, $J = 4.7$ Hz, 1H, thiophene-H), 7.30 (d, $J = 2.6$ Hz, 1H, thiophene-H), 7.22 (d, $J = 8.7$ Hz, 2H, Ar-H), 7.12 (t, $J = 3.8$ Hz, 1H, thiophene-H), 6.95 (d, $J = 8.7$ Hz, 2H, Ar-H), 5.31 (t, $J = 9.7$ Hz, 1H, $-\text{CH}_X$), 4.07–3.89 (m, 2H, $-\text{NCH}_2$), 3.82 (dd, $J = 17.0, 12.6$ Hz, 1H, $-\text{CH}_A\text{H}$), 3.12 (dd, $J = 17.2, 9.3$ Hz, 1H, $-\text{CH}_B\text{H}$), 2.22 (s, 3H, pyrrole $-\text{CH}_3$), 2.13 (s, 3H, pyrrole $-\text{CH}_3$); HRMS (ESI) calcd. for $[\text{M}+\text{H}]^+$ $\text{C}_{22}\text{H}_{21}\text{ClF}_3\text{N}_4\text{O}_5^+$: 481.1076, found: 481.1076.

5-[1-Acetyl-3-(thiophen-2-yl)-4,5-dihydro-1H-pyrazol-5-yl]-2,4-dimethyl-N-(2,2,2-trifluoroethyl)-1H-pyrrole-3-carboxamide (15i)

The product was obtained as an off-white solid; yield: 0.52 g, 89.9%; R_F (mobile phase hexanes/EtOAc 50:50): 0.30; m.p.: 221–223°C; ^1H NMR (500 MHz, DMSO- d_6): δ 10.74 (s, 1H, $-\text{NH}$), 7.73 (t, $J = 4.7$ Hz, 2H, thiophene-H, $-\text{CONH}$), 7.44 (d, $J = 3.1$ Hz, 1H, thiophene-H), 7.16 (t, $J = 4.2$ Hz, 1H, thiophene-H), 5.47 (dd, $J = 12.1, 6.0$ Hz, 1H, $-\text{CH}_X$), 4.05–3.87 (m, 2H, $-\text{NCH}_2$), 3.78 (dd, $J = 17.7, 12.5$ Hz, 1H, $-\text{CH}_A\text{H}$), 3.13 (dd, $J = 17.8, 6.1$ Hz, 1H, $-\text{CH}_B\text{H}$), 2.22 (s, 3H, $-\text{NCOCH}_3$), 2.18 (s, 3H, pyrrole $-\text{CH}_3$), 2.03 (s, 3H, pyrrole $-\text{CH}_3$); HRMS (ESI) calcd. for $[\text{M}+\text{H}]^+$ $\text{C}_{18}\text{H}_{20}\text{F}_3\text{N}_4\text{O}_5\text{S}^+$: 413.1259, found: 413.1252.

5-[1-(Cyclobutanecarbonyl)-3-(thiophen-2-yl)-4,5-dihydro-1H-pyrazol-5-yl]-2,4-dimethyl-N-(2,2,2-trifluoroethyl)-1H-pyrrole-3-carboxamide (15j)

The product was obtained as an off-white solid; yield: 0.56 g, 88.2%; R_F (mobile phase hexanes/EtOAc 50:50): 0.40; m.p.: 231–233°C; ^1H NMR (400 MHz, DMSO- d_6): δ 10.75 (s, 1H, $-\text{NH}$), 7.82–7.71 (m, 2H, $-\text{CONH}$, thiophene-H), 7.42 (t, $J = 3.5$ Hz, 1H, thiophene-H), 7.15 (d, $J = 5.0$ Hz, 1H, thiophene-H), 5.44 (dd, $J = 15.0, 7.5$ Hz, 1H, $-\text{CH}_X$), 4.00–3.92 (m, 2H, $-\text{NCH}_2$), 3.73 (m, 2H, $-\text{COCH}$, $-\text{CH}_A\text{H}$), 3.11 (dd, $J = 22.5, 9.3$ Hz, 1H, $-\text{CH}_B\text{H}$), 2.19 (s, 3H, pyrrole $-\text{CH}_3$), 2.14 (m, 4H, $-\text{CH}_A\text{H}(\text{CH}_2)\text{CH}_A\text{H}$), 2.02 (s, 3H, pyrrole $-\text{CH}_3$), 1.93 (dd, $J = 18.3, 9.3$ Hz, 1H, $-\text{COCCH}_B\text{H}$), 1.73 (m, 1H, $-\text{COCCH}_B\text{H}$); HRMS (ESI) calcd. for $[\text{M}+\text{H}]^+$ $\text{C}_{21}\text{H}_{24}\text{F}_3\text{N}_4\text{O}_5\text{S}^+$: 453.1572, found: 453.1578.

5-[3-[3-Fluoro-4-(trifluoromethyl)phenyl]-1-methyl-4,5-dihydro-1H-pyrazol-5-yl]-2,4-dimethyl-N-(2,2,2-trifluoroethyl)-1H-pyrrole-3-carboxamide (15k)

The product was obtained as an off-white solid; yield: 0.47 g, 88.3%; R_F (mobile phase hexanes/EtOAc 50:50): 0.70; m.p.: 167–169°C; ^1H NMR (500 MHz, DMSO- d_6): δ 10.94 (s, 1H, $-\text{NH}$), 7.89–7.71 (m, 2H, Ar-H, $-\text{CONH}$), 7.64 (t, $J = 9.6$ Hz, 2H, Ar-H), 4.32 (dd, $J = 14.9, 10.5$ Hz, 1H, $-\text{CH}_X$), 4.10–3.88 (m, 2H, $-\text{NCH}_2$), 3.41 (dd, $J = 16.4, 10.5$ Hz, 1H, $-\text{CH}_A\text{H}$), 3.03 (t, $J = 15.7$ Hz, 1H, $-\text{CH}_B\text{H}$), 2.73 (s, 3H, $-\text{NCH}_3$), 2.28 (s, 3H, pyrrole $-\text{CH}_3$), 2.08 (s, 3H, pyrrole $-\text{CH}_3$); ^{13}C NMR (126 MHz, DMSO- d_6): δ 166.68, 160.60, 158.61, 146.85, 140.24, 130.68, 128.84, 128.08, 126.62, 126.43, 124.40, 124.27, 122.94, 122.18, 122.11, 121.90, 119.94, 116.88, 115.45, 113.60, 113.43, 64.08, 40.62, 38.83, 12.83, 10.26; HRMS (ESI) calcd. for $[\text{M}+\text{H}]^+$ $\text{C}_{20}\text{H}_{20}\text{F}_7\text{N}_4\text{O}^+$: 465.1525, found: 465.1528.

5-[3-[3-Fluoro-4-(trifluoromethyl)phenyl]-1-phenyl-4,5-dihydro-1H-pyrazol-5-yl]-2,4-dimethyl-N-(2,2,2-trifluoroethyl)-1H-pyrrole-3-carboxamide (15l)

The product was obtained as an off-white solid; yield: 0.49 g, 81.2%; R_F (mobile phase hexanes/EtOAc 50:50): 0.70; m.p.: 191–193°C; ^1H NMR (500 MHz, DMSO- d_6): δ 10.89 (s, 1H, $-\text{NH}$), 8.10–7.56 (m, 4H, Ar-H, $-\text{CONH}$), 7.34–7.00 (m, 4H, Ar-H), 6.81 (t, $J = 6.7$ Hz, 1H, Ar-H), 5.45 (t, $J = 10.3$ Hz, 1H, $-\text{CH}_X$), 3.97 (dd, $J = 15.1, 10.1$ Hz, 2H, $-\text{NCH}_2$), 3.81 (dd, $J = 16.8, 13.4$ Hz, 1H, $-\text{CH}_A\text{H}$), 3.13 (dd, $J = 17.3, 8.9$ Hz, 1H, $-\text{CH}_B\text{H}$), 2.22 (s, 3H, pyrrole $-\text{CH}_3$), 2.13 (s, 3H, pyrrole $-\text{CH}_3$); HRMS (ESI) calcd. for $[\text{M}+\text{H}]^+$ $\text{C}_{25}\text{H}_{22}\text{F}_7\text{N}_4\text{O}^+$: 527.1682, found: 527.1686.

5-[1-(4-Chlorophenyl)-3-[3-fluoro-4-(trifluoromethyl)phenyl]-4,5-dihydro-1H-pyrazol-5-yl]-2,4-dimethyl-N-(2,2,2-trifluoroethyl)-1H-pyrrole-3-carboxamide (15m)

The product was obtained as an off-white solid; yield: 0.49 g, 76.2%; R_F (mobile phase hexanes/EtOAc 60:40): 0.50; m.p.: 139–143°C; ^1H NMR (500 MHz, DMSO- d_6): δ 10.88 (s, 1H, $-\text{NH}$), 7.79 (m, 4H, $-\text{CONH}$, Ar-H), 7.24 (dd, $J = 8.5, 3.0$ Hz, 2H, Ar-H), 7.08 (dd, $J = 8.5, 3.0$ Hz, 2H, Ar-H), 5.48 (dd, $J = 16.0, 10.5$ Hz, 1H, $-\text{CH}_X$), 4.02–3.91 (m, 2H, $-\text{NCH}_2$), 3.82 (dd, $J = 22.0, 16.0$ Hz, 1H, $-\text{CH}_A\text{H}$), 3.13 (dd, $J = 22.5, 11.0$ Hz, 1H, $-\text{CH}_B\text{H}$), 2.21 (s, 3H, pyrrole $-\text{CH}_3$), 2.11 (s, 3H, pyrrole $-\text{CH}_3$); HRMS (ESI) calcd. for $[\text{M}+\text{H}]^+$ $\text{C}_{25}\text{H}_{21}\text{ClF}_7\text{N}_4\text{O}^+$: 561.1292, found: 561.1294.

5-[1-Acetyl-3-[3-fluoro-4-(trifluoromethyl)phenyl]-4,5-dihydro-1H-pyrazol-5-yl]-2,4-dimethyl-N-(2,2,2-trifluoroethyl)-1H-pyrrole-3-carboxamide (15n)

The product was obtained as an off-white solid; yield: 0.48 g, 85.1%; R_F (mobile phase hexanes/EtOAc 50:50): 0.20; m.p.: 285–287°C; ^1H NMR (500 MHz, DMSO- d_6): δ 10.72 (s, 1H, $-\text{NH}$), 7.92–7.72 (m, 4H, Ar-H, $-\text{CONH}$), 5.52 (dd, $J = 15.5, 7.5$ Hz, 1H, $-\text{CH}_X$), 4.05–3.92 (m, 2H, $-\text{NCH}_2$), 3.78 (dd, $J = 22.5, 15.5$ Hz, 1H, $-\text{CH}_A\text{H}$), 3.16 (dd, $J = 23.0, 7.5$ Hz, 1H, $-\text{CH}_B\text{H}$), 2.22 (s, 6H, $-\text{NCOCH}_3$, pyrrole $-\text{CH}_3$), 2.03 (s, 3H, pyrrole $-\text{CH}_3$); ^{13}C NMR (126 MHz, DMSO- d_6): δ 168.28,

166.70, 160.52, 158.50, 152.09, 138.92, 129.75, 128.83, 128.27, 126.61, 125.95, 124.39, 124.09, 123.30, 122.16, 121.93, 115.45, 115.31, 115.13, 52.82, 40.48, 22.34, 12.76, 10.30; HRMS (ESI) calcd. for $[M+H]^+$ $C_{21}H_{20}F_7N_4O_2^+$: 493.1474, found: 493.1473.

5-[1-Acetyl-3-[3-fluoro-4-(trifluoromethyl)phenyl]-4,5-dihydro-1H-pyrazol-5-yl]-2,4-dimethyl-N-(2,2,2-trifluoroethyl)-1H-pyrrole-3-carboxamide (**15o**)

The product was obtained as an off-white solid; yield: 0.51 g, 83.6%; R_f (mobile phase hexanes/EtOAc 50:50): 0.60; m.p.: 259–261°C; 1H NMR (400 MHz, DMSO- d_6): δ 10.73 (s, 1H, -NH), 7.92–7.72 (m, 4H, -CONH, Ar-H), 5.50 (dd, $J = 16.0, 8.0$ Hz, 1H, -CH $_X$), 4.02–3.80 (m, 2H, -NCH $_2$), 3.76 (m, 2H, -COCH, -CH $_A$ H), 3.13 (dd, $J = 23.0, 10.5$ Hz, 1H, -CH $_B$ H), 2.20 (s, 3H, pyrrole -CH $_3$), 2.15 (m, 4H, -CH $_A$ H(CH $_2$)CH $_A$ H), 2.03 (s, 3H, pyrrole -CH $_3$), 1.94 (dq, $J = 18.3, 9.6$ Hz, 1H, -COCCH $_B$ H), 1.74 (m, 1H, -COCCH $_B$ H); ^{13}C NMR (126 MHz, DMSO- d_6): δ 172.29, 166.70, 160.53, 158.51, 151.87, 139.03, 129.80, 128.83, 128.27, 126.61, 126.19, 126.06, 124.39, 124.10, 123.23, 122.17, 121.94, 119.78, 115.43, 115.25, 115.14, 53.07, 37.92, 25.22, 24.75, 18.16, 12.78, 10.21; HRMS (ESI) calcd. for $[M+H]^+$ $C_{24}H_{24}F_7N_4O_2^+$: 533.1787, found: 533.1787.

4.2 | Biological assays

4.2.1 | In vitro antibacterial assay

A sample of each cultured bacterium was diluted 40-fold in fresh broth and incubated at 37°C for 1.5–3 hr. The resultant mid-log phase cultures were diluted (CFU/ml measured by OD600) and then added to each well of the compound containing plates, giving a cell density of 5×10^5 CFU/ml and a total volume of 50 μ l. Covered plates were incubated at 37°C for 18 hr without shaking. The inhibition of bacterial growth was determined by measuring absorbance at 600 nm (OD600), using a Tecan M1000 Pro monochromator plate reader. The % GI was calculated for each well, using the negative control (media only) and positive control (bacteria without inhibitors) on the same plate as references.

4.2.2 | In vitro antifungal assay

Fungi strains were cultured for 3 days on yeast extract, peptone, and dextrose (YPD) agar at 30°C. A yeast suspension of 1×10^6 to 5×10^6 CFU/ml (as determined by OD530) was prepared from five colonies. The suspension was subsequently diluted and added to each well of the compound-containing plates giving a final cell density of fungi suspension of 2.5×10^3 CFU/ml and a total volume of 50 μ l. All covered plates were incubated at 35°C for 24 hr without shaking. The GI of *C. albicans* was determined by measuring absorbance at 530 nm (OD530), whereas the GI of *C. neoformans* was determined by measuring the difference in absorbance between 600 and 570 nm (OD600–570), after the addition of resazurin (0.001% final concentration) and incubation at 35°C for an additional 2 hr. The absorbance was measured using a Biotek

Synergy HTX plate reader. The percentage of GI was calculated for each well, using negative control (media only) and positive control (fungi without inhibitors) on the same plate.

4.2.3 | In vitro anticancer assay

All demonstrated compounds were submitted to National Cancer Institute (NCI), Bethesda, MD, and they were further evaluated for their antiproliferative activity at the concentration of 10 μ M in DMSO on a panel of 60 cancer cell lines as per the standard protocol of NCI. The solution of each compound was added to the microtiter culture plates and kept for the incubation for 48 hr at 37°C. The endpoint of testing was determined using a protein-binding dye, that is, sulforhodamine B. The growth percentage of each treated cell was determined by comparison with the untreated control cells and the collective result was reported at the NCI website.

4.2.4 | In vitro cytotoxicity assay

The counted HEK293 cells in a Neubauer hemocytometer were plated in the 384-well plates containing the compounds to give a density of 5,000 cells/well in a final volume of 50 μ l. Dulbecco's modified Eagle's medium supplemented with 10% fetal bovine serum (FBS) was used as growth media. Along with the compounds, HEK293 cells were incubated for 20 hr at 37°C in 5% CO $_2$. Cytotoxicity was measured by fluorescence, ex: 560/10 nm, em: 590/10 nm (F560/590), after the addition of 5 μ l of 25 μ g/ml resazurin (2.3 μ g/ml final concentration) and after incubation for further 3 hr at 37°C in 5% CO $_2$. The fluorescence intensity was measured using a Tecan M1000 Pro monochromator plate reader, using automatic gain calculation. CC $_{50}$ values were calculated by curve fitting the inhibition values versus log (concentration) using a sigmoidal dose-response function, with variable fitting values for the bottom, top, and slope. Cytotoxic samples were analyzed in duplicate.

4.2.5 | Hemolysis assay

The human whole blood was washed three times by three volumes of 0.9% sodium chloride solution and then suspended in the same to a concentration of 0.5×10^8 cells/ml by calculating in a Neubauer hemocytometer. The washed cells were then added to 384-well plates containing the compound for a final volume of 50 μ l. First, the plates were shaken on a plate shaker for 10 min and then incubated for 1 hr at 37°C. After incubation, the plates were centrifuged at 1,000 g for 10 min to pellet cells and debris, and 25 μ l of the supernatant was then transferred to a polystyrene 384-well assay plate. HC $_{10}$ and HC $_{50}$ (concentration at 10% and 50% hemolysis, respectively) were calculated by curve fitting the inhibition values versus log (concentration) using a sigmoidal dose-response function with variable fitting values for top, bottom, and slope. Hemolysis samples were analyzed in duplicate.

4.3 | Molecular docking

A molecular docking study was performed by downloading Protein Data Bank file 4AGD (resolution: 2.81 Å). Docking simulation was employed using AutoDock Vina on PyRx,^[43] whereas visualization of the docking results was performed by the Discovery Studio program following the standard procedure.

ACKNOWLEDGMENTS

The authors thank the Baburaoji Gholap Research Center for its support, the Central Instrumental Facility (CIF) at Savitribai Phule Pune University and the Indian Institute of Science Education and Research (IISER), Pune for its analytical support. They are also thankful to the Developmental Therapeutics Program, NCI, for in vitro anticancer evaluation and CO-ADD, which was funded by the Wellcome Trust (UK), and The University of Queensland (Australia) for cytotoxicity and hemolysis assay.

CONFLICTS OF INTERESTS

The authors declare that there are no conflicts of interests.

ORCID

Sangeeta V. Jagtap  <http://orcid.org/0000-0002-5947-1013>

REFERENCES

- [1] V. F. Roche *Foye's Principles of Medicinal Chemistry*, 7th ed. (Eds: T. L. Lemke, D. A. Williams, V. F. Roche, S. W. Zito), Williams & Wilkins, Walter Kluwer Health, Baltimore and Philadelphia **2013**, Ch.37.
- [2] R. L. Siegel, K. D. Miller, A. Jemal, *CA: Cancer J. Clin.* **2016**, *66*, 7.
- [3] World Health Organization, Newsroom, <https://www.who.int/cancer/PRGloboCanFinal.pdf> (accessed: April 2020).
- [4] P. G. Corrie, *Medicine* **2008**, *36*, 24.
- [5] K. Lv, L. L. Wang, M. L. Liu, X. B. Zhou, S. Y. Fan, H. Y. Liu, Z. B. Zheng, S. Li, *Bioorg. Med. Chem. Lett.* **2011**, *21*, 3062.
- [6] Y. Z. Jin, D. X. Fu, N. Ma, Z. C. Li, Q. H. Liu, L. Xiao, R. H. Zhang, *Molecules* **2011**, *16*, 9368.
- [7] H. S. Ibrahim, S. M. Abou-Seri, H. A. Abdel-Aziz, *Eur. J. Med. Chem.* **2016**, *122*, 366.
- [8] J. V. Mehta, S. B. Gajera, P. Thakor, V. R. Thakkar, M. N. Patel, *RSC Adv.* **2015**, *5*, 85350.
- [9] A. Burmuđžija, Z. Ratković, J. Muškinja, N. Janković, B. Ranković, M. Kosanić, S. Dorđević, *RSC Adv.* **2016**, *6*, 91420.
- [10] V. K. Mishra, M. Mishra, V. Kashaw, S. K. Kashaw, *Bioorg. Med. Chem.* **2017**, *25*, 1949.
- [11] J. Ramírez-Prada, S. M. Robledo, I. D. Vélez, M. del P. Crespo, J. Quiroga, R. Abonia, A. Montoya, L. Svetaz, S. Zacchino, B. Insuasty, *Eur. J. Med. Chem.* **2017**, *131*, 237.
- [12] D. Havrylyuk, B. Zimenkovsky, O. Vasylenko, C. W. Day, D. F. Smee, P. Grellier, R. Lesyk, *Eur. J. Med. Chem.* **2013**, *66*, 228.
- [13] S. C. Karad, V. B. Purohit, P. Thakor, V. R. Thakkar, D. K. Raval, *Eur. J. Med. Chem.* **2016**, *112*, 270.
- [14] D. N. Rana, M. T. Chhabria, N. K. Shah, P. S. Brahmshatriya, *Med. Chem. Res.* **2014**, *23*, 2218.
- [15] G. Mótyán, F. Kovács, J. Wölfling, A. Gyovai, I. Zupkó, É. Frank, *Steroids* **2016**, *112*, 36.
- [16] M. A. Abdel-Sayed, S. M. Bayomi, M. A. El-Sherbeny, N. I. Abdel-Aziz, K. E. H. Eltahir, G. S. G. Shehatou, A. A. M. Abdel-Aziz, *Bioorg. Med. Chem.* **2016**, *24*, 2032.
- [17] M. S. Muneera, J. Joseph, *J. Photochem. Photobiol., B* **2016**, *163*, 57.
- [18] M. Amir, H. Kumar, S. A. Khan, *Bioorg. Med. Chem. Lett.* **2008**, *18*, 918.
- [19] Y. Lee, B. S. Kim, S. Ahn, D. Koh, Y. H. Lee, S. Y. Shin, Y. Lim, *Bioorg. Chem.* **2016**, *68*, 166.
- [20] S. Y. Shin, S. Ahn, H. Yoon, H. Jung, Y. Jung, D. Koh, Y. H. Lee, Y. Lim, *Bioorg. Med. Chem. Lett.* **2016**, *26*, 4301.
- [21] R. S. Joshi, P. G. Mandhane, S. D. Diwakar, S. K. Dabhade, C. H. Gill, *Bioorg. Med. Chem. Lett.* **2010**, *20*, 3721.
- [22] P. L. Zhao, W. Fu, M. Z. Zhang, Z. M. Liu, H. Wei, G. F. Yang, *J. Agric. Food Chem.* **2008**, *56*, 10767.
- [23] B. Liu, S. Yan, L. Qu, J. Zhu, *Cancer Cell. Int.* **2017**, *17*, 1.
- [24] J. Li, Q. Hao, W. Cao, J. V. Vadgama, Y. Wu, *Cancer Manag. Res.* **2018**, *10*, 4653.
- [25] R. F. George, M. Kandeel, D. Y. El-Ansary, A. M. El Kerdawy, *Bioorg. Chem.* **2020**, *99*, 103780.
- [26] X. X. Tao, Y. T. Duan, L. W. Chen, D. J. Tang, M. R. Yang, P. F. Wang, C. Xu, H. L. Zhu, *Bioorg. Med. Chem. Lett.* **2016**, *26*, 677.
- [27] S. Y. Shin, H. Yoon, D. Hwang, S. Ahn, D. W. Kim, D. Koh, Y. H. Lee, Y. Lim, *Bioorg. Med. Chem.* **2013**, *21*, 7018.
- [28] K. M. Amin, S. M. Abou-Seri, F. M. Awadallah, A. A. M. Eissa, G. S. Hassan, M. M. Abdulla, *Eur. J. Med. Chem.* **2015**, *90*, 221.
- [29] Y. J. Qin, Y. jing Li, A. Q. Jiang, M. R. Yang, Q. Z. Zhu, H. Dong, H. L. Zhu, *Eur. J. Med. Chem.* **2015**, *94*, 447.
- [30] N. K. Rasal, R. B. Sonawane, A. S. Choudhari, S. S. Chakraborty, D. D. Sarkar, S. V. Jagtap, *ChemistrySelect* **2018**, *3*, 9571.
- [31] N. K. Rasal, R. B. Sonawane, S. V. Jagtap, *Bioorg. Chem.* **2020**, *97*, 103660.
- [32] L. Sun, C. Liang, S. Shirazian, Y. Zhou, T. Miller, J. Cui, J. Y. Fukuda, J. Y. Chu, A. Nematalla, X. Wang, H. Chen, A. Sistla, T. C. Luu, F. Tang, J. Wei, C. Tang, *J. Med. Chem.* **2003**, *46*, 1116.
- [33] M. A. T. Blaskovich, J. Zuegg, A. G. Elliott, M. A. Cooper, *ACS Infect. Dis.* **2016**, *1*, 285.
- [34] National Cancer institute, Development Therapeutic program, <http://www.nci.nih.gov> (accessed: March 2020).
- [35] M. R. Grever, S. A. Schepartz, B. A. Chabner, *Semin. Oncol.* **1992**, *19*, 622.
- [36] A. Monks, D. Scudiero, P. Skehan, R. Shoemaker, K. Paull, D. Vistica, C. Hose, J. Langley, P. Cronise, A. Vaigro-Wolff, M. Gray-Goodrich, H. Campbell, J. Mayo, M. Boyd, *J. Natl. Cancer Inst.* **1991**, *83*, 757.
- [37] M. R. Boyd, K. D. Paull, *Drug Dev. Res.* **1995**, *34*, 91.
- [38] C. A. Lipinski, *Drug Discov. Today: Technol.* **2004**, *1*, 337.
- [39] A. Daina, O. Michielin, V. Zoete, *Sci. Rep.* **2017**, *7*, 42717.
- [40] A. Daina, O. Michielin, V. Zoete, *J. Chem. Inf. Model.* **2014**, *54*, 3284.
- [41] A. Daina, V. Zoete, *ChemMedChem* **2016**, *11*, 1117.
- [42] A. M. Grimaldi, T. Guida, R. D'Attino, E. Perrotta, M. Otero, A. Masala, G. Carteni, *Ann. Oncol.* **2007**, *18*, vi31.
- [43] O. Trott, A. J. Olson, *J. Comput. Chem.* **2010**, *31*, 455.

SUPPORTING INFORMATION

Additional supporting information may be found online in the Supporting Information section.

How to cite this article: Rasal NK, Sonawane RB, Jagtap SV. Synthesis, biological evaluation, and in silico study of pyrazoline-conjugated 2,4-dimethyl-1H-pyrrole-3-carboxylic acid derivatives. *Arch Pharm.* 2020;e2000267. <https://doi.org/10.1002/ardp.202000267>